Shootin1 interacts with actin retrograde flow and L1-CAM to promote axon outgrowth

Tadayuki Shimada,[1] Michinori Toriyama,[1] Kaori Uemura,[1] Hiroyuki Kamiguchi,[3] Tadao Sugiura,[2] Naoki Watanabe,[4] and Naoyuki Inagaki[1]

[1]Division of Signal Transduction and [2]Biomedical Imaging and Informatics, Nara Institute of Science and Technology, Ikoma 630-0192, Japan
[3]Laboratory for Neuronal Growth Mechanisms, Brain Science Institute, Institute of Physical and Chemical Research (RIKEN), Saitama 351-0198, Japan
[4]Department of Pharmacology, Kyoto University Faculty of Medicine, Kyoto 606-8501, Japan

Actin polymerizes near the leading edge of nerve growth cones, and actin filaments show retrograde movement in filopodia and lamellipodia. Linkage between actin filament retrograde flow and cell adhesion molecules (CAMs) in growth cones is thought to be one of the mechanisms for axon outgrowth and guidance. However, the molecular basis for this linkage remains elusive. Here, we show that shootin1 interacts with both actin filament retrograde flow and L1-CAM in axonal growth cones of cultured rat hippocampal neurons, thereby mediating the linkage between them. Impairing this linkage, either by shootin1 RNA interference or disturbing the interaction between shootin1 and actin filament flow, inhibited L1-dependent axon outgrowth, whereas enhancing the linkage by shootin1 overexpression promoted neurite outgrowth. These results strengthen the actin flow–CAM linkage model ("clutch" model) for axon outgrowth and suggest that shootin1 is a key molecule involved in this mechanism.

Introduction

The nerve growth cone is the migrating tip of growing neurites and plays a central role in axon outgrowth and guidance (Ramon y Cajal, 1890; Bray and Hollenbeck, 1988). Actin polymerizes near the leading edge of growth cones, and actin filaments show remarkable retrograde movement in filopodia and lamellipodia (Forscher and Smith, 1988; Katoh et al., 1999; Mallavarapu and Mitchison, 1999). Myosin 1c and myosin II have been implicated in actin filament retrograde flow in growth cones (Diefenbach et al., 2002; Medeiros et al., 2006). Linkage between the actin filament retrograde flow and cell adhesion molecules (CAMs) is thought to transmit the force of actin filament movement to extracellular substrates via CAMs (Mitchison and Kirschner, 1988; Jay, 2000; Suter and Forscher, 2000), thereby providing mechanical tension (Bray, 1979; Lamoureux et al., 1989) and protrusion of the leading edge (Lin and Forscher, 1995) for axon outgrowth and steering. Previous studies demonstrated that CAMs such as apCAM (Suter et al., 1998), Nr-CAM (Faivre-Sarrailh et al., 1999), integrin (Grabham et al., 2000), and L1-CAM (Kamiguchi and Yoshihara, 2001) are coupled with actin filament retrograde flow in growth cones. Consistently, coupling between apCAM and actin filament retrograde flow produced mechanical tension and induced protrusion of growth cones (Suter et al., 1998).

L1 is a single-pass transmembrane protein expressed predominantly in developing neurons and involved in axon outgrowth and guidance (Lemmon et al., 1989; Dahme et al., 1997; Kamiguchi et al., 1998). A recent study showed that ankyrin$_B$ promotes neurite initiation by coupling F-actin flow to L1 (Nishimura et al., 2003). However, ankyrin$_B$ was involved neither in their coupling in growth cones nor in L1-mediated neurite elongation, and the molecular basis for the actin flow–CAM linkage in growth cones remains elusive (Suter et al., 1998; Gil et al., 2003; Nishimura et al., 2003). It is also unanswered whether coupling of this linkage is involved in the regulation of axon outgrowth. Recently we described a novel brain-specific intracellular protein, shootin1, which is involved in axon formation and polarization of cultured hippocampal neurons (Toriyama et al., 2006). Shootin1 accumulates in axonal growth cones, and its accumulation in growth cones dynamically enhances neurite elongation. Shootin1 was shown to act upstream of phosphoinositide-3-kinase

Correspondence to N. Inagaki: ninagaki@bs.naist.jp

Abbreviations used in this paper: CAM, cell adhesion molecule; DIC, differential interference contrast; NES, nuclear export signal; PI 3-kinase, phosphoinositide-3-kinase; shRNA, short hairpin RNA.

The online version of this paper contains supplemental material.

The Rockefeller University Press $30.00
J. Cell Biol. Vol. 181 No. 5 817–829
www.jcb.org/cgi/doi/10.1083/jcb.200712138

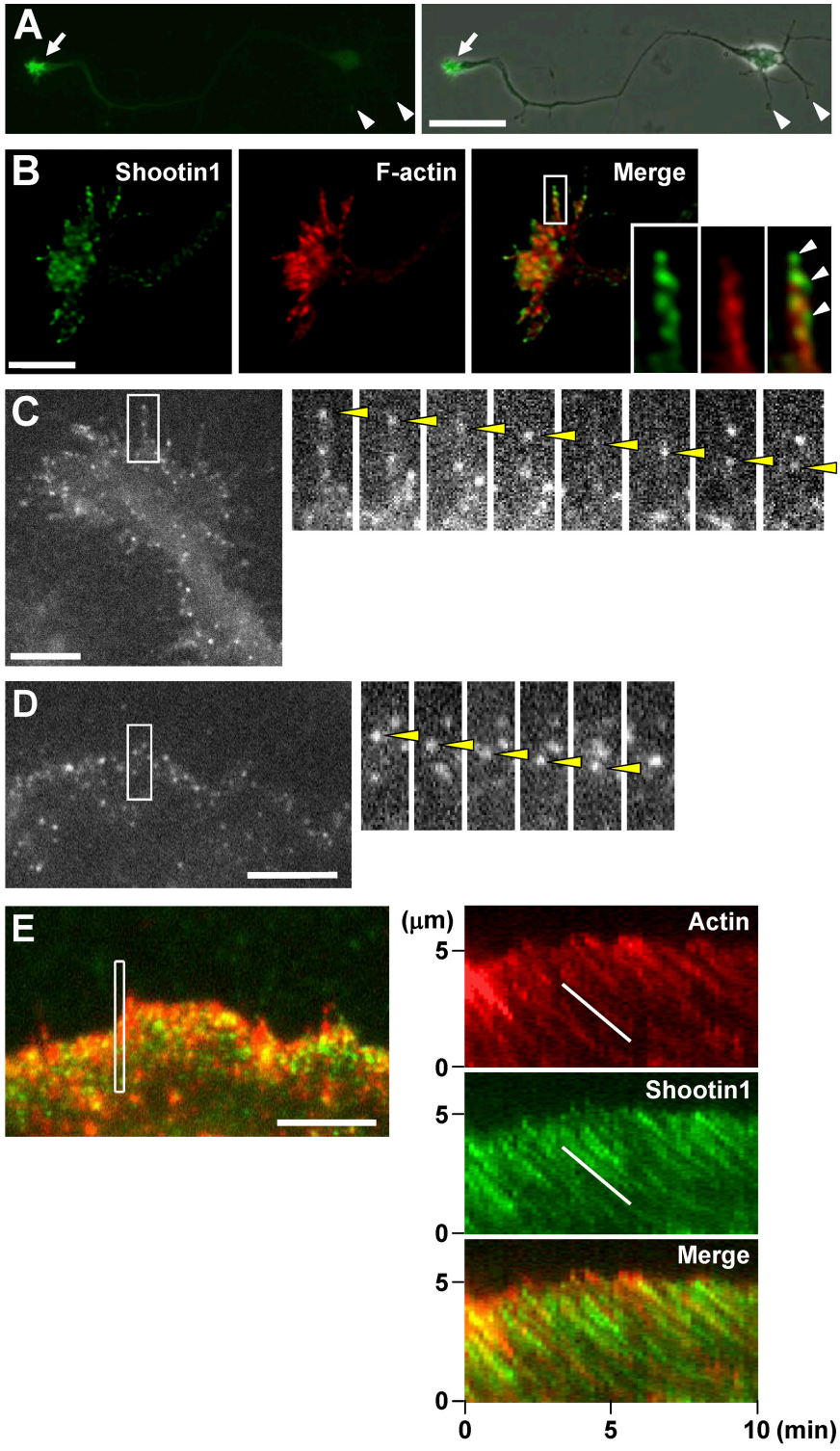

Figure 1. **Shootin1 and actin filaments in axonal growth cones and XTC fibroblasts.** (A) Immunofluorescent localization of shootin1 in a cultured hippocampal neuron. Arrows and arrowheads denote an axonal growth cone and minor process growth cones, respectively. (B) Deconvolved images of an axonal growth cone stained by anti-shootin1 antibody and rhodamine phalloidin. (inset) An enlarged view of the filopodium in the rectangle. Arrowheads indicate shootin1 accumulation in a filopodium. (C) A fluorescent speckle image of EGFP-shootin1 in an axonal growth cone (left) and time series of the indicated area at 5-s intervals (right). See Video 1 (available at http://www.jcb.org/cgi/content/full/jcb.200712138/DC1). (D) A fluorescent speckle image of EGFP-shootin1 expressed in an XTC fibroblast (left) and a time series of the indicated area at 10-s intervals (right). See Video 2. Yellow arrowheads denote a speckle of EGFP-shootin1 moving retrogradely. (E) A fluorescent speckle image of mCherry-β-actin (red) and EGFP-shootin1 (green) coexpressed in an XTC fibroblast (left). See Video 3. The kymographs (right) of the peripheral region indicated by the rectangle in the left panel show that the speckles of shootin1 and those of actin retrograde flow moved at similar speeds (lines). Bar: (A) 50 μm; (B–E) 5 μm.

(PI 3-kinase). However, shootin1-induced axon formation was not fully suppressed by a PI 3-kinase inhibitor (Toriyama et al., 2006), which suggests the existence of an additional mechanism for axon outgrowth. Here, we show that shootin1 interacts with both actin filament retrograde flow and L1-CAM in growth cones. Our data suggest that shootin1 mediates the linkage between actin retrograde flow and L1-CAM to promote axon outgrowth.

Results

Shootin1 interacts with both actin filament retrograde flow and L1-CAM in growth cones

Fig. 1 A shows shootin1 immunoreactivity in a cultured rat hippocampal neuron. Shootin1 accumulated to a high level in axonal growth cones (Fig. 1 A, arrows), where it localized

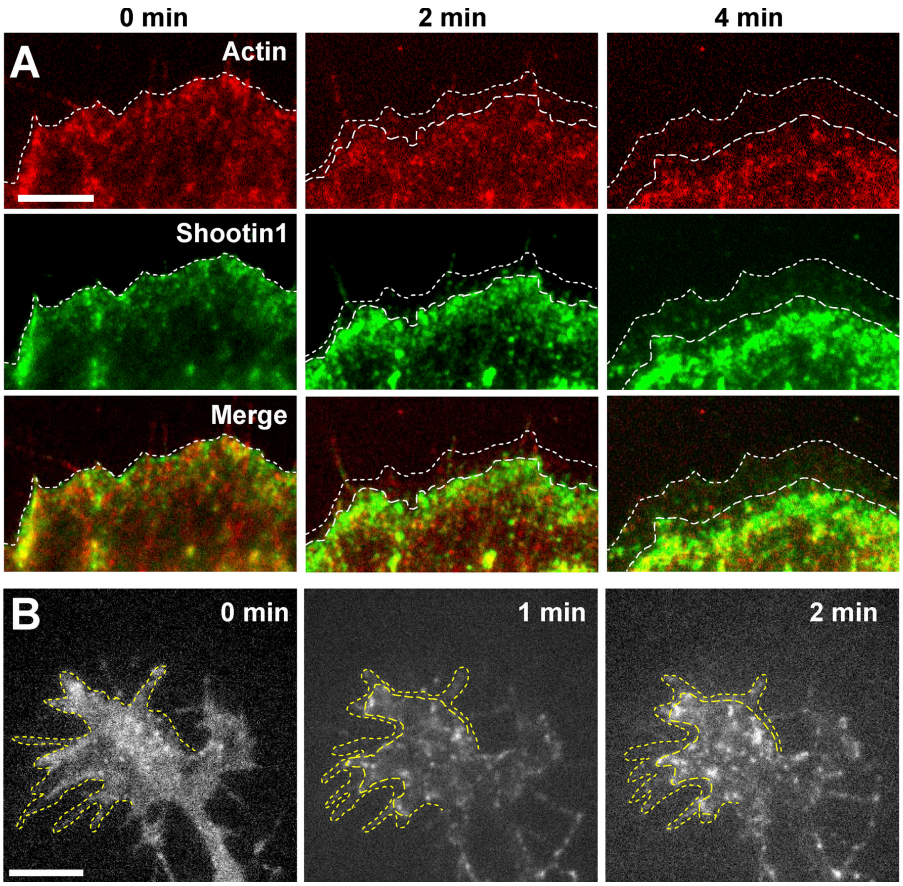

Figure 2. **Effect of cytochalasin D on retrograde movement of EGFP-shootin1 speckles in XTC fibroblasts and axonal growth cones.** (A) Time-lapse speckle images of mCherry–β-actin (red) and EGFP-shootin1 (green) coexpressed in XTC fibroblasts treated with 1 µM cytochalasin D at 0 min. See Video 4 (available at http://www.jcb.org/cgi/content/full/jcb.200712138/DC1). (B) Time-lapse speckle images of EGFP-shootin1 in an axonal growth cone treated with 1 µM cytochalasin D at 0 min. See Video 5. Dotted lines indicate the leading edge and boundary of speckles. Bars, 5 µm.

in filopodia and lamellipodia in close apposition with actin filaments (Fig. 1 B, arrowheads). To elucidate the association of shootin1 with cytoskeletal dynamics in growth cones, we performed fluorescent speckle microscopy (Waterman-Storer and Salmon, 1997; Watanabe and Mitchison, 2002). We performed live imaging of EGFP-shootin1 expressed at a low level in cultured hippocampal neurons. EGFP-shootin1 appeared as discrete speckle signals that serve as fiduciary marks, allowing measurement of molecular movement of shootin1. Shootin1 speckles displayed retrograde movement in filopodia and lamellipodia of axonal growth cones (Fig. 1 C, arrowheads; and Video 1, available at http://www.jcb.org/cgi/content/full/jcb.200712138/DC1). The mean speed of shootin1 speckles was 4.5 ± 0.4 µm/min (mean ± SD, n = 60), which is similar to that of actin filament retrograde flow in axonal growth cones (Katoh et al., 1999; Mallavarapu and Mitchison, 1999) and fibroblast lamellipodia (Watanabe and Mitchison, 2002).

To compare the movement of shootin1 speckles directly with that of actin filament retrograde flow, we coexpressed EGFP-shootin1 and β-actin fused to mCherry (Shaner et al., 2004) in XTC fibroblasts, which are suitable for speckle imaging of actin retrograde flow in lamellipodia (Watanabe and Mitchison, 2002). EGFP-shootin1 signals also showed retrograde movement in lamellipodia of XTC fibroblasts (Fig. 1 D, arrowheads; and Video 2, available at http://www.jcb.org/cgi/content/full/jcb.200712138/DC1). Speckles of EGFP-shootin1 and those of mCherry-actin retrograde flow moved at similar speeds (EGFP-shootin1: 2.6 ± 0.9 µm/min, n = 20; mCherry-actin: 2.7 ± 0.5 µm/min, n = 20; Fig. 1 E and Video 3), which suggests that shootin1 interacts with actin filament retrograde flow. To confirm this, we inhibited actin polymerization near the leading edge of lamellipodia with cytochalasin. As previously described (Forscher and Smith, 1988; Medeiros et al., 2006), treatment of XTC fibroblasts with 1 µM cytochalasin D led to disruption of the peripheral regions of actin filament networks in lamellipodia. The boundary of the mCherry-actin speckles moved from the leading edge of lamellipodia at 1.3 ± 0.3 µm/min (n = 10), and the flow speed of actin speckles was reduced to 0.9 ± 0.1 µm/min (n = 10; Fig. 2 A and Video 4). Concurrently, the boundary of EGFP-shootin1 speckles moved rearward at the same rate (1.2 ± 0.4 µm/min, n = 10) and the speed of shootin1 speckles was also reduced to 1.0 ± 0.1 µm/min (n = 10), thereby indicating that the signals of shootin1 coincide with the redistribution of actin filament networks. Similar rearward movement of the boundary of EGFP-shootin1 speckles and a reduction of the speed of shootin1 speckles were also induced by cytochalasin D in filopodia and lamellipodia of axonal growth cones (Fig. 2 B and Video 5). We conclude from these observations that shootin1 interacts dynamically with actin filaments, which move retrogradely in axonal growth cones.

L1 is a single-pass transmembrane protein expressed predominantly in developing neurons and involved in axon outgrowth and guidance (Lemmon et al., 1989; Dahme et al., 1997; Kamiguchi et al., 1998). L1 immunoreactivity localized in axonal growth cones of hippocampal neurons, in close apposition

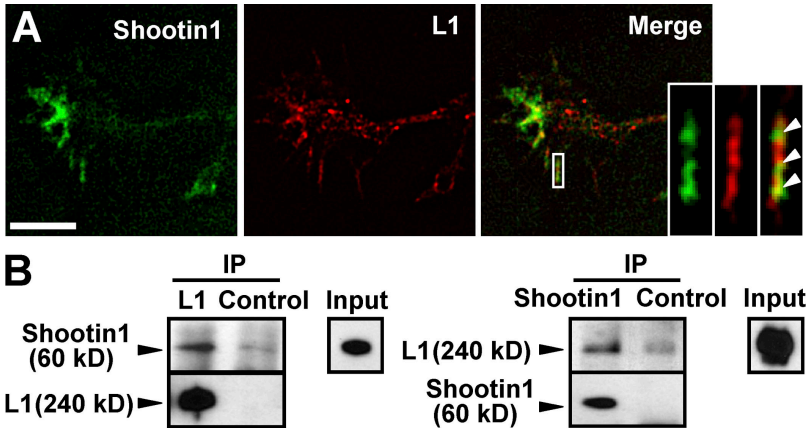

Figure 3. **Shootin1 associates with L1.** (A) Deconvolved images of an axonal growth cone stained by anti-shootin1 and anti-L1 antibodies. (inset) An enlarged view of the rectangle. Arrowheads indicate shootin1 accumulation in a filopodium. Bar, 5 µm. (B) Coimmunoprecipitation of shootin1 and L1 from P5 rat brain lysates. Brain lysates were incubated with anti-shootin1 antibody, anti-L1 antibody, or control IgG. The immunoprecipitates were analyzed by immunoblotting with anti-shootin1 and anti-L1 antibodies.

with shootin1 (Fig. 3 A, arrowheads). We examined the physiological association between shootin1 and L1 by coimmunoprecipitation assay. When shootin1 was immunoprecipitated from P5 rat brain lysates, coprecipitation of L1 was detected; shootin1 was also reciprocally coimmunoprecipitated with L1 (Fig. 3 B). We also coexpressed exogenous shootin1 and L1 in HEK293T cells but could not detect coimmunoprecipitation between shootin1 and L1 (unpublished data). These results indicate that shootin1 associates with L1 in vivo, probably through unidentified neuron-specific proteins.

L1 is linked to actin filament retrograde flow in growth cones of hippocampal neurons

By tracking the movement of microbeads coated with L1-Fc, which binds homophilically to L1, or anti-L1 antibody, a previous study showed that L1 is linked to actin filament retrograde flow in growth cones of chick dorsal root ganglion neurons (Kamiguchi and Yoshihara, 2001). Microbeads coated with L1-Fc, anti-L1 antibody, or IgG (control) were placed on axonal growth cones of hippocampal neurons cultured on coverslips coated with N-cadherin–Fc using laser optical tweezers. Similar to the case of dorsal root ganglion neurons (Kamiguchi and Yoshihara, 2001), 54% of the beads coated with L1-Fc showed retrograde directional movement (n = 24; Fig. S1, A and B, available at http://www.jcb.org/cgi/content/full/jcb.200712138/DC1), whereas the remaining 46% showed Brownian motion or no movement. The mean velocity of the moving beads was 1.1 ± 0.10 µm/min (mean ± SEM). Similar results were obtained with beads coated with anti-L1 antibody (n = 25; Fig. S1 B). However, only 32% of the IgG-coated beads showed retrograde movement (n = 25), and the velocity of the moving beads (0.64 ± 0.08 µm/min) was significantly slower than that of beads coated with L1-Fc or anti-L1 antibody (P = 0.0030 compared with L1-Fc; P = 0.00012 compared with anti-L1 antibody; Fig. S1 B). In addition, none of the L1-Fc–coated beads showed retrograde movement in the presence of both 1 µM cytochalasin D and 50 µM blebbistatin (n = 23; unpublished data), which block actin filament retrograde movement (Medeiros et al., 2006). Together, these results indicate that L1 is linked to actin filament retrograde flow in the axonal growth cones of hippocampal neurons.

Shootin1 mediates the linkage between actin filament retrograde flow and L1 in growth cones

To examine whether shootin1 mediates this linkage, we first suppressed shootin1 expression in hippocampal neurons using short hairpin RNA (shRNA). Neurons expressing shRNA against shootin1 were immunostained by anti-shootin1 antibody after the observation of actin filament retrograde flow in growth cones (Fig. S2, A and B, available at http://www.jcb.org/cgi/content/full/jcb.200712138/DC1). The mean shootin1 immunoreactivity in growth cones of neurons expressing the shRNA (n = 6 growth cones) was 11% of that in growth cones expressing the control shRNA (n = 6 growth cones). The rates of EGFP-actin retrograde flow in growth cones expressing shootin1 shRNA and in those expressing control shRNA were 4.0 ± 0.9 µm/min (n = 60) and 4.1 ± 0.5 µm/min (n = 60), respectively; the difference between them was not significant (P = 0.91). In addition, there was no significant difference in the levels and organization of actin filaments in growth cones expressing shootin1 shRNA and those expressing control shRNA (n = three independent cultures, 150 growth cones examined; P = 0.27; Fig. S2 C).

However, suppression of shootin1 by shRNA significantly reduced the flow velocity of L1-Fc–coated beads (n = 71, P = 0.0000035 compared with control; Fig. 4, A, B, and E; and Videos 6 and 7, available at http://www.jcb.org/cgi/content/full/jcb.200712138/DC1), although it did not affect the percentage of the beads that showed retrograde flow. The peak velocity of moving beads declined substantially from 0.8–1.0 µm/min to 0.4–0.6 µm/min. In addition, expression of an RNAi refractory myc-shootin1 rescued the effect of shootin1 RNAi (n = 44; P = 0.85 compared with control; P = 0.00024 compared with RNAi; Fig. 4, C–E). Each L1-Fc–coated bead probably binds to multiple L1 molecules in growth cones, thereby monitoring the engagement of multiple L1 molecules with actin filament retrograde flow. Thus, the reduction in the flow velocity of L1-Fc–coated beads by RNAi without a change in the actin filament retrograde flow rate suggests that suppression of shootin1 in growth cones reduces the number of L1 molecules linked to actin flow. We do not rule out the alternative possibility that L1 can bind to F-actin flow weakly even in the absence of shootin1. In such a case, shootin1 down-regulation would lead to a

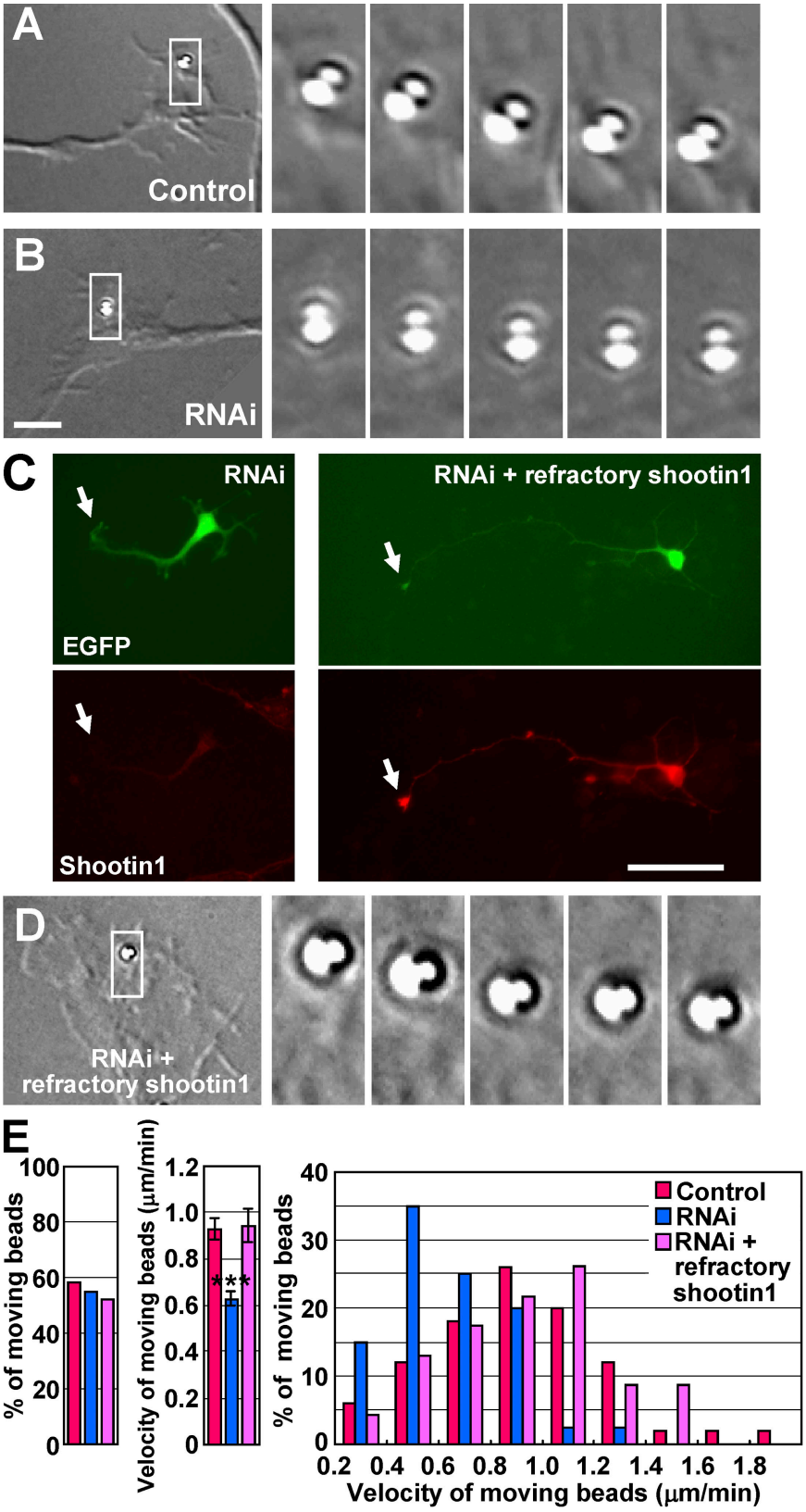

Figure 4. **Repression of shootin1 expression by RNAi weakens the actin flow–L1 linkage.** (A, B, and D) DIC micrographs showing retrograde movement of L1-Fc–coated beads on axonal growth cones (two days in vitro) expressing a control shRNA (A), the shRNA designated against shootin1 (B), or the shRNA designated against shootin1 together with the mutant myc-shootin1 (D), which is refractory to the shRNA (left), and time series of the indicated areas at 30-s intervals (right). See Videos 6 and 7 (available at http://www.jcb.org/cgi/content/full/jcb.200712138/DC1). As previously described (Toriyama et al., 2006), about half of the RNAi-induced neurons polarized after 48 h in vitro. Therefore, we selected such neurons and performed the analysis on their axonal growth cones. (C) Hippocampal neurons transfected with shootin1 shRNA (left), or shootin1 shRNA together with the refractory myc-shootin1 (right) were cultured for 48 h. The vector to express the shRNAs is designed to coexpress EGFP (green). Shootin1 and myc-shootin1 were immunostained by anti-shootin1 (left) and anti-myc (right) antibodies, respectively (red). Arrows denote axonal growth cones. (E) The percentage of beads coated with L1-Fc that showed retrograde flow on growth cones expressing a control shRNA (n = 86), shootin1 shRNA (n = 71), or shootin1 shRNA and the refractory myc-shootin1 (n = 44); mean velocity of moving beads as means ± SEM (***, $P < 0.0005$ compared with control and RNAi + refractory shootin1); and the percentage of moving beads with indicated velocities. Bars: (B) 5 μm; (C) 50 μm.

decrease in the number of L1 molecules strongly linked to F-actin flow. Concerning the percentage of the moving beads, Gil et al. (2003) found that the stationary behavior of beads bound to cell surface L1 is mediated by ankyrin. The percentage of moving L1-Fc–coated beads may therefore be mainly regulated by this molecule. Together, these results suggest that shootin1 mediates the linkage between actin filament retrograde flow and L1 in growth cones.

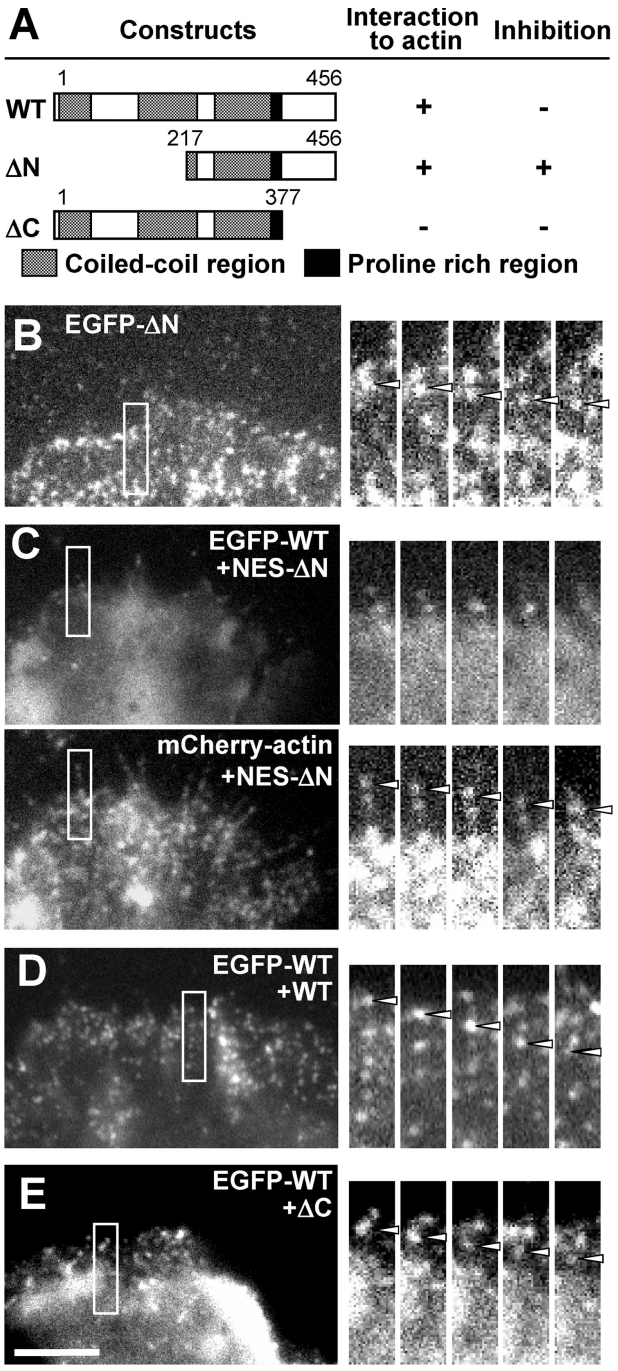

Figure 5. **NES-ΔN-shootin1 disturbs the linkage between shootin1 and actin filament retrograde flow.** (A) Schematic representation of the wild-type (WT) and ΔN- and ΔC-shootin1, and their abilities to interact with actin filament flow and inhibit the interaction between EGFP-shootin1 and actin filament flow. Numbers indicate amino acid numbers. (B and C) Fluorescent speckle images of EGFP-ΔN-shootin1 (B, left), and EGFP-shootin1 and mCherry-actin coexpressed in the same XTC fibroblast (C, left), with a time series of the indicated area of the cells at 10-s intervals (right). Myc-NES-ΔN-shootin1 was also overexpressed in the cell in C under the β-actin promoter. See Videos 8 and 9 (available at http://www.jcb.org/cgi/content/full/jcb.200712138/DC1). (D and E) Fluorescent speckle images of EGFP-shootin1 (left) in XTC fibroblasts and a time series of the indicated area of the cells at 10-s intervals (right). Myc-shootin1 (D) and myc-ΔC-shootin1 (E) were also overexpressed in the cells under the β-actin promoter. Arrowheads indicate speckles of EGFP-ΔN-shootin1 (B), mCherry-actin (C), and EGFP-shootin1 (D and E) moving retrogradely. Bar, 5 μm.

ΔN-shootin1 and NES-ΔN-shootin1 disturb the interaction between shootin1 and actin filament retrograde flow

Next, we designed a shootin1 deletion mutant that disturbs the interaction between shootin1 and actin filament flow. Because shootin1 does not have well-characterized functional domains (Toriyama et al., 2006), we could not design mutants based on domain structure. ΔN-shootin1 was produced by deleting the N-terminal 216 amino acids from the wild type (Fig. 5 A). We fused the nuclear export signal (NES) LSLKLAGLDL (Fukuda et al., 1996) to the N terminus of ΔN-shootin1, as ΔN-shootin1 unexpectedly accumulated in the neuronal nucleus. Myc-NES-ΔN-shootin1 was localized in the cytoplasm of hippocampal neurons and accumulated in growth cones (unpublished data). When EGFP-ΔN-shootin1 or EGFP-NES-ΔN-shootin1 were expressed in XTC fibroblasts, their speckles showed retrograde movement similar to that of EGFP-shootin1 (Fig. 5 B and Video 8, available at http://www.jcb.org/cgi/content/full/jcb.200712138/DC1; and data not shown), which suggests that these mutants also interact with actin filament retrograde flow. Overexpression of myc-NES-ΔN-shootin1 in XTC cells decreased the number of EGFP-shootin1 speckles that displayed retrograde movement without affecting the retrograde flow of mCherry-actin speckles (Fig. 5 C and Video 9). Similar results were obtained for myc-ΔN-shootin1 (unpublished data). We also produced ΔC-shootin1, in which the C-terminal 79 amino acids of the wild type were deleted (Fig. 5 A). In contrast to ΔN-shootin1, EGFP-ΔC-shootin1 did not interact with actin retrograde filament flow in XTC cells (Fig. 5 A), and myc-ΔC-shootin1 did not accumulate in neuronal growth cones (not depicted). In addition, overexpression of myc-shootin1 or myc-ΔC-shootin1 in XTC cells did not decrease substantially the number of EGFP-shootin1 speckles that displayed retrograde movement (Fig. 5, D and E). These results suggest that ΔN-shootin1 and NES-ΔN-shootin1 disturb the interaction between shootin1 and actin filament retrograde flow.

Myc-NES-ΔN-shootin1 was overexpressed in hippocampal neurons to disturb this interaction. The rates of EGFP-actin retrograde flow in growth cones overexpressing myc-NES-ΔN-shootin1 and in those overexpressing the control protein myc-GST were 3.6 ± 0.4 μm/min ($n = 60$) and 3.9 ± 0.4 μm/min ($n = 60$), respectively (Fig. S2, D and E); the difference between them was not significant ($P = 0.12$). In addition, there was no significant difference between the levels and organization of actin filaments in growth cones expressing these proteins (n = three independent cultures, 150 growth cones examined; $P = 0.48$; Fig. S2 F). However, overexpression of myc-NES-ΔN-shootin1 decreased the percentage of L1-Fc–coated beads that showed retrograde flow on axonal growth cones and significantly reduced the velocity of the retrograde flow ($n = 41$, $P = 0.011$ compared with myc-GST; Fig. 6, A–C). The peak velocity of moving beads declined substantially from 0.8–1.0 μm/min to 0.4–0.6 μm/min, which suggests that disturbing the shootin1-actin flow interaction also weakens the actin flow–L1 linkage. These results suggest that disturbing the interaction between shootin1 and actin filament flow by NES-ΔN-shootin1 also impairs the actin flow–L1 linkage, and strengthen the notion that shootin1 mediates the linkage between actin filament retrograde flow and L1 in growth cones.

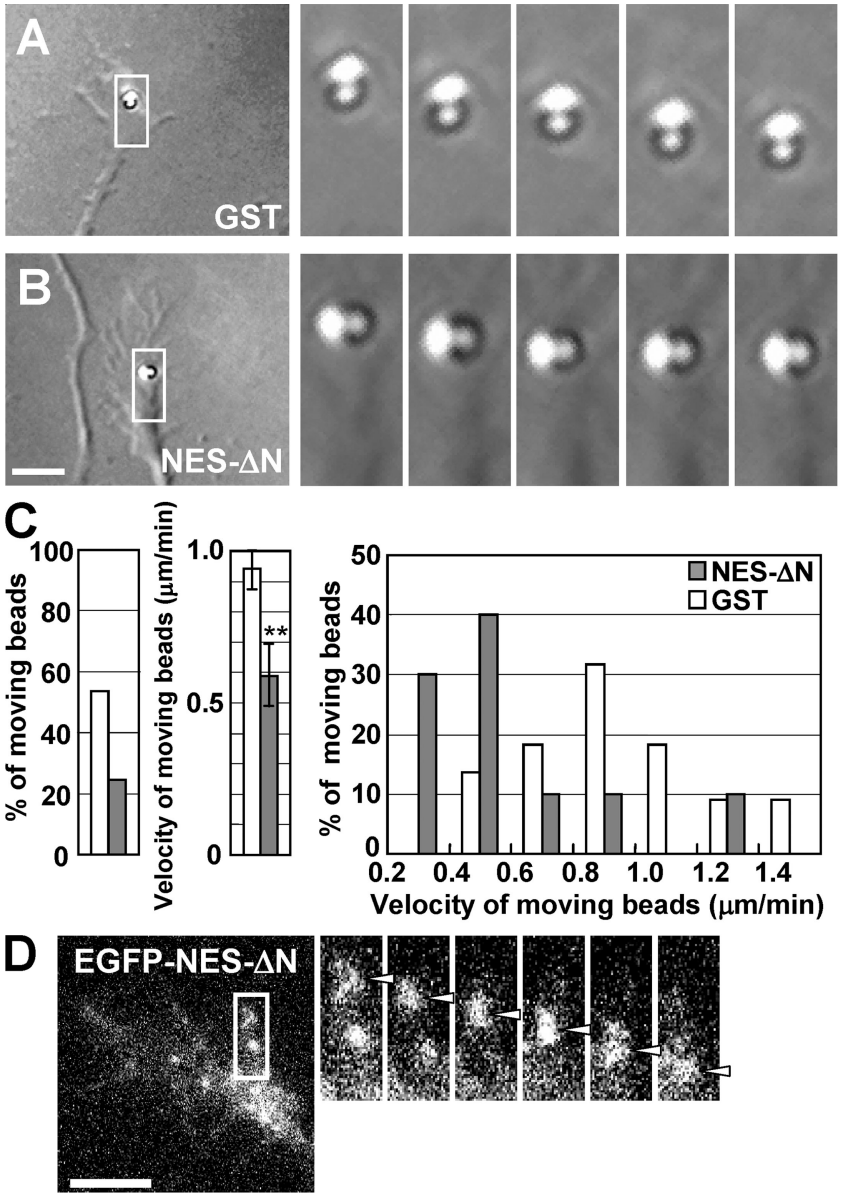

Figure 6. **Disturbing the linkage between shootin1 and actin filament retrograde flow by NES-ΔN-shootin1 weakens the actin flow–L1 linkage.** (A and B) DIC micrographs showing retrograde movement of L1-Fc–coated beads on axonal growth cones (two days in vitro) overexpressing myc-GST (A, left) or myc-NES-ΔN-shootin1 (B, left), and a time series of the indicated areas at 30-s intervals (A and B, right). (C) The percentage of beads coated with L1-Fc that showed retrograde flow on growth cones expressing myc-GST (n = 41) or myc-NES-ΔN-shootin1 (n = 41), mean velocity of moving beads as means ± SEM (**, P < 0.02), and the percentage of moving beads with indicated velocities. (D) A fluorescent speckle image of EGFP-NES-ΔN-shootin1 in an axonal growth cone (left) and a time series of the indicated area at 5-s intervals (right). Arrowheads indicate a speckle of EGFP-NES-ΔN-shootin1 moving retrogradely. Bars, 5 μm.

To examine whether NES-ΔN-shootin1 retains the ability to associate with L1, we compared the flow speeds of EGFP-NES-ΔN-shootin1 (Fig. 6 D) and EGFP-shootin1 (Fig. 1 C) in growth cones: they were 4.2 ± 0.5 μm/min (mean ± SD, n = 60) and 4.5 ± 0.4 μm/min (mean ± SD, n = 60), respectively, and not significantly different (P = 0.37). Together with the finding that overexpression of myc-NES-ΔN-shootin1 reduced the velocity of the L1-Fc-coated beads, these observations suggested that ΔN-shootin1 has a reduced ability to associate with L1.

Impairing the actin flow–L1 linkage by shootin1 RNAi inhibits L1-dependent axon outgrowth

Next, we analyzed the effects of impairing the actin flow–L1 linkage on axon outgrowth. Hippocampal neurons were transfected with shRNA against shootin1 and cultured for 48 h on coverslips coated with L1-Fc or a control substrate, polylysine. As has been described (Oliva et al., 2003), control neurons developed longer axons on L1-Fc than on polylysine (Fig. 7, A and B), which suggests that homophilic binding between L1 in growth cones and L1-Fc on culture plates is important for axon outgrowth. Suppression of shootin1 expression by RNAi resulted in a significant decrease in axonal length on L1-Fc (n = three independent cultures, 160 neurons examined; P = 0.0086 compared with control; Fig. 7 B), whereas shootin1 RNAi on polylysine caused only a marginal reduction of axonal length (n = three independent cultures, 174 neurons examined; P = 0.22 compared with control). The decrease in axonal length by RNAi was significantly smaller on polylysine than on L1-Fc (P = 0.032; Fig. 7 C). This is consistent with the observation that shootin1 RNAi reduced the velocity of retrograde movement of L1-Fc–coated beads on axonal growth cones (Fig. 4) but did not affect the movement of polylysine-coated beads (n = 49; P = 0.58 compared with control; Fig. 8, A–C). The inhibition of axon elongation on L1-Fc by RNAi was rescued by expression of the RNAi refractory myc-shootin1 (n = three independent cultures,

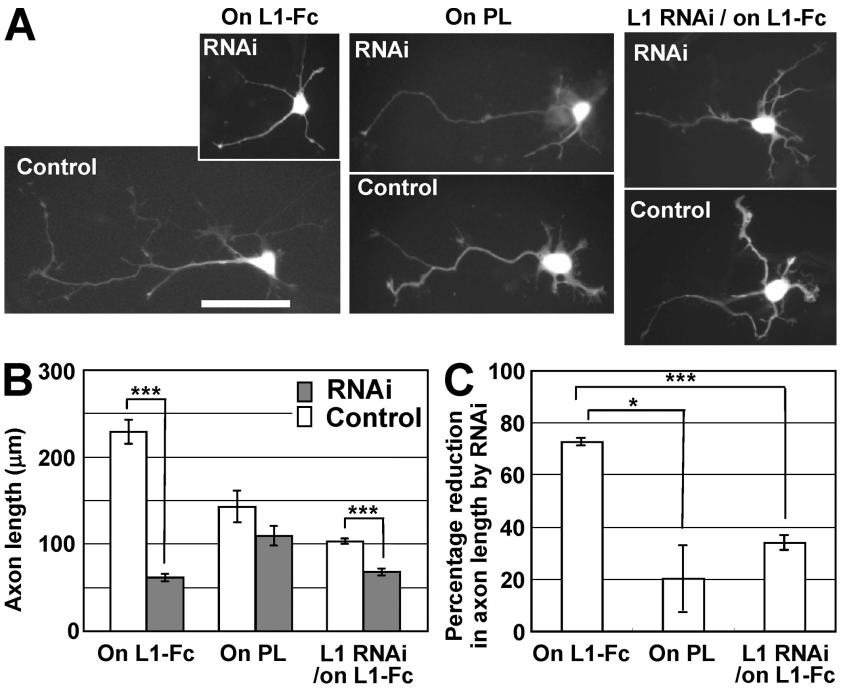

Figure 7. **Impairing the actin flow–L1 linkage by RNAi inhibits L1-dependent axon outgrowth.** Hippocampal neurons were transfected with shRNA against shootin1 or with control shRNA, and cultured on L1-Fc– or polylysine-coated coverslips for 48 h. Some were also cotransfected with shRNA against L1. Neuronal morphology was visualized by EGFP fluorescence. (A) Vectors expressing shRNAs coexpress EGFP. (B) Length of axons or the longest neurites. (C) The percentage reduction in axons by shootin1 RNAi (mean ± SEM; *, $P < 0.05$, ***, $P < 0.01$; $n = 3$ independent cultures; 512 neurons were examined). Bar, 50 μm.

270 neurons examined; P = 0.60 compared with control; P = 0.00068 compared with RNAi; Fig. S3 A, available at http://www.jcb.org/cgi/content/full/jcb.200712138/DC1).

To further confirm that these RNAi effects are L1 dependent, neurons were cotransfected with shRNA against L1 and cultured on L1-Fc. Consistent with the notion that homophilic binding between L1 in growth cones and L1-Fc on culture plates is important for axon outgrowth, neurons transfected with control shRNA and cultured on L1-Fc developed longer axons than those transfected with L1 shRNA and cultured on L1-Fc (Fig. 7, A and B).

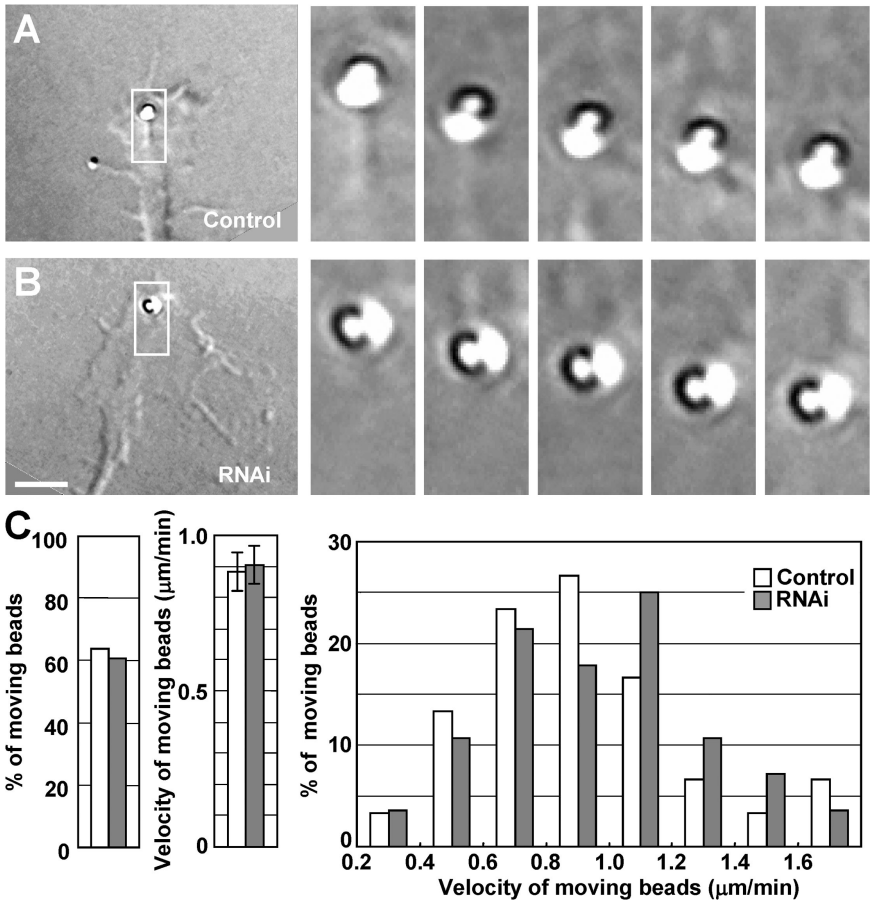

Figure 8. **Shootin1 RNAi does not affect the movement of polylysine-coated beads on axonal growth cones.** (A and B) DIC micrographs showing retrograde movement of polylysine-coated beads on axonal growth cones (two days in vitro) expressing a control shRNA (A, left) or a shRNA against shootin1 (B, left), and a time series of the indicated areas at 30-s intervals (A and B, right). (C) The percentage of polylysine-coated beads that showed retrograde flow on axonal growth cones expressing the control ($n = 46$) or shootin1 shRNA ($n = 49$), mean velocity of moving beads as means ± SEM, and the percentage of moving beads with indicated velocities. Bar, 5 μm.

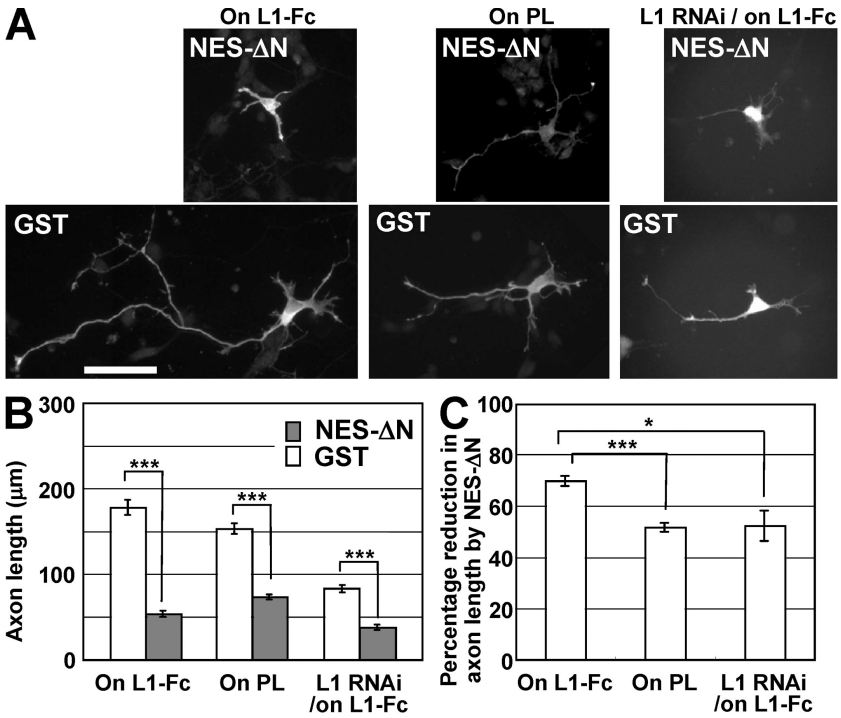

Figure 9. **Impairing the actin flow–L1 linkage by myc-NES-ΔN-shootin1 inhibits L1-dependent axon outgrowth.** Neurons overexpressing myc-NES-ΔN-shootin1 or myc-GST were cultured on L1-Fc– or polylysine-coated coverslips for 48 h and stained by anti-myc antibody (A). Some were cotransfected with shRNA against L1. (B) The lengths of axons or the longest neuritis. (C) The percentage reduction in axons by expressing myc-NES-ΔN-shootin1 (mean ± SEM; *, P < 0.05, ***, P < 0.01; *n* = 3 independent cultures, 1,370 neurons were examined). Bar, 50 μm.

Shootin1 RNAi reduced axonal length of neurons transfected with L1 shRNA and cultured on L1-Fc (*n* = three independent cultures, 178 neurons examined; P = 0.0022 compared with control; Fig. 7, A and B), though to a significantly lesser degree than the reduction seen in neurons without L1 RNAi (P = 0.00063; Fig. 7 C), thereby confirming the L1-dependency of the RNAi effects. We previously found that shootin1-induced axon formation was inhibited by the PI-3 kinase inhibitor LY294002 (Toriyama et al., 2006). However, it was not fully suppressed, which suggests the existence of an additional PI-3 kinase–independent mechanism for shootin1-induced axon outgrowth. Therefore, we also examined whether the effects of shootin1 RNAi on L1-dependent axon outgrowth are affected by PI 3-kinase activity. In the presence of 20 μM LY294002, shootin1 RNAi resulted in a significant decrease in axon outgrowth on L1-Fc (*n* = three independent cultures, 226 neurons examined; P = 0.00015 compared with control) but not on polylysine (*n* = three independent cultures, 213 neurons examined; P = 0.52 compared with control; Fig. S3 B). The decrease in axon outgrowth by shootin1 RNAi on L1-Fc in the presence or absence of LY294002 was similar (P = 0.73; Fig. S3C), thereby suggesting that the effects of shootin1 RNAi on L1-dependent axon outgrowth are not influenced by PI 3-kinase activity. Together, these results suggest that impairing the actin flow–L1 linkage by shootin1 RNAi inhibits L1-dependent axon outgrowth.

Impairing the actin flow–L1 linkage by NES-ΔN-shootin1 inhibits L1-dependent axon outgrowth

Next, we examined the effects of disturbing the actin flow–shootin1 linkage by NES-ΔN-shootin1 on axon outgrowth. As in the case of shootin1 RNAi, overexpression of myc-NES-ΔN-shootin1 in hippocampal neurons also reduced axon outgrowth significantly on L1-Fc (*n* = three independent cultures, 623 neurons examined; P = 0.00083 compared with GST; Fig. 9, A and B). We noted that cell bodies of some neurons overexpressing myc-NES-ΔN-shootin1 showed a rather flattened morphology (unpublished data). Overexpressing myc-NES-ΔN-shootin1 in neurons cultured on polylysine or in neurons expressing L1 shRNA also inhibited axon outgrowth (for neurons on polylysine: *n* = three independent cultures, 565 neurons examined, P = 0.0062 compared with GST; for neurons expressing L1 shRNA: *n* = three independent cultures, 182 neurons examined, P = 0.00088 compared with GST; Fig. 9, A and B); however, the effects were significantly weaker than those in neurons cultured on L1-Fc without L1 RNAi (for neurons on polylysine: P = 0.0014; for neurons expressing L1 shRNA: P = 0.034; Fig. 9 C). Thus, although these data suggest an additional L1-independent effect of myc-NES-ΔN-shootin1, it also inhibited L1-dependent axon outgrowth.

Enhancing the actin flow–L1 linkage by shootin1 overexpression promotes L1-dependent neurite outgrowth

Finally, we examined whether increased levels of shootin1 alter the linkage between actin flow and L1. To do so, because shootin1 accumulates strongly in axonal growth cones (Fig. 1 A, arrows; Toriyama et al., 2006), we monitored the movement of actin retrograde flow and L1-Fc–coated beads on minor process growth cones, where shootin1 levels are low (Fig. 1 A, arrowheads). The rates of EGFP-actin retrograde flow in growth cones overexpressing myc-shootin1 and in those overexpressing myc-GST were 4.6 ± 0.8 μm/min (*n* = 60) and 4.3 ± 0.5 μm/min (*n* = 60), respectively (Fig. S4, A and B, available at http://www.jcb.org/cgi/content/full/jcb.200712138/DC1); the difference between them was not significant (P = 0.25). In addition, there

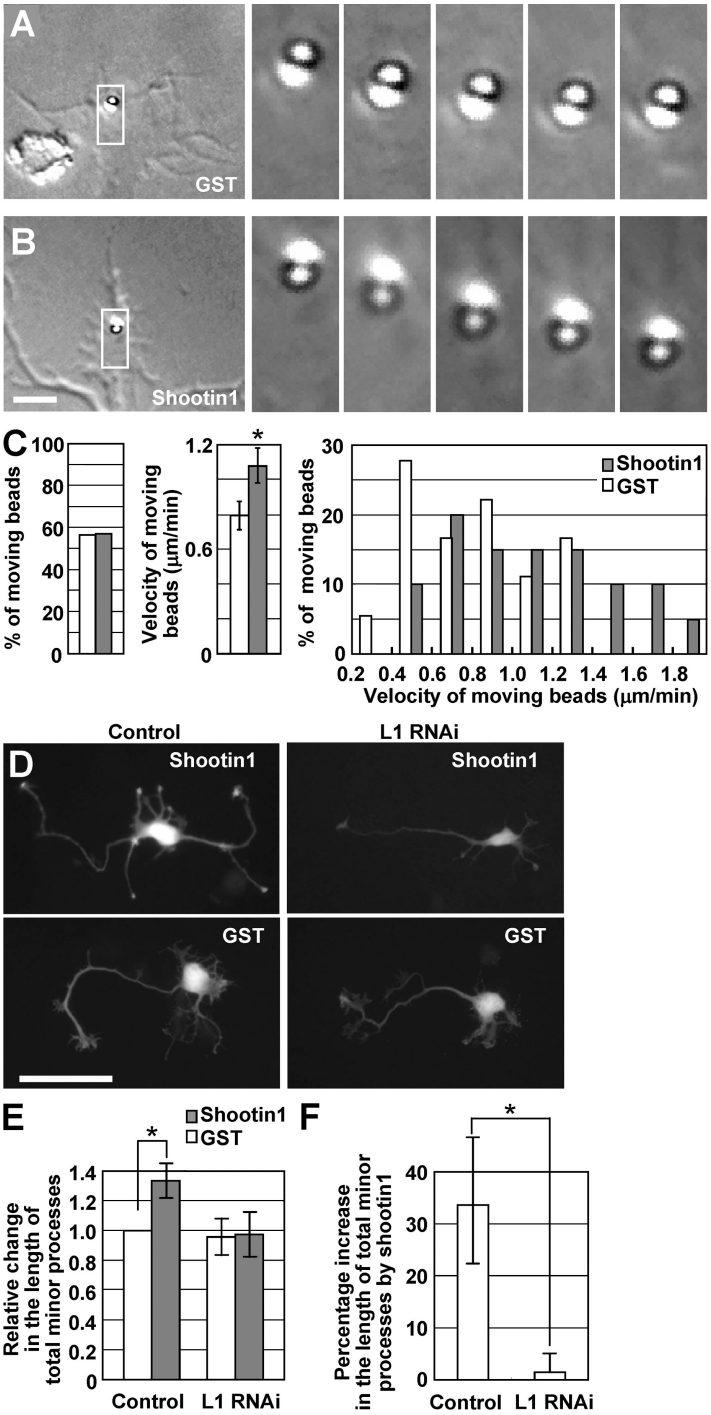

Figure 10. **Enhancing the actin flow–L1 linkage by shootin1 overexpression promotes L1-dependent neurite outgrowth.** (A and B) DIC micrographs showing retrograde movement of L1-Fc–coated beads on minor process growth cones (one day in vitro) overexpressing myc-GST (A, left) or myc-shootin1 (B, left), and a time series of the indicated areas at 30-s intervals (A and B, right). (C) The percentage of beads coated with L1-Fc that showed retrograde flow on minor process growth cones expressing myc-GST (n = 28) or myc-shootin1 (n = 35), mean velocity of moving beads as means ± SEM (*, $P < 0.05$), and the percentage of moving beads with indicated velocities. (D–F) Neurons overexpressing myc-shootin1 or myc-GST were cultured on L1-Fc–coated coverslips for 24 h (D). They were also cotransfected with control shRNA or shRNA against L1. (E) The lengths of total minor processes (lengths of all neurites except the longest one) relative to that of the control neurons expressing myc-GST and control shRNA. (F) The percentage increase in total minor processes upon expression of myc-shootin1 (mean ± SEM; *, $P < 0.05$; n = 4 independent cultures, 554 neurons were examined). Bars: (B), 5 μm; (D) 50 μm.

was no significant difference between the levels and organization of actin filaments in growth cones expressing these proteins (n = three independent cultures, 150 growth cones examined; P = 0.42; Fig. S4 C).

In contrast to shootin1 RNAi and myc-NES-ΔN-shootin1 overexpression, myc-shootin1 overexpression significantly increased the velocity of those beads that showed retrograde movement on minor process growth cones (n = 35, P = 0.045 compared with GST; Fig. 10, A–C), which suggests that it enhanced the actin flow–L1 linkage. These results further strengthen the notion that shootin1 mediates the linkage between actin filament retrograde flow and L1 in growth cones. Concurrently, myc-shootin1 overexpression in hippocampal neurons promoted outgrowth of total minor processes on L1-Fc (n = four independent cultures, 276 neurons examined; P = 0.039 compared with GST; Fig. 10, D and E) but not in neurons expressing shRNA against L1 (n = four independent cultures, 278 neurons examined; P = 0.47 compared with GST; Fig. 10, D–F). We also examined whether the effects of shootin1 overexpression on L1-dependent neurite outgrowth are affected by PI 3-kinase activity. In the presence of LY294002, shootin1 overexpression resulted in a significant increase in axonal length on L1-Fc (n = 3

independent cultures, 244 neurons examined; P = 0.050 compared with control; Fig. S4 D). A similar increase was observed in the absence of LY294002 (P = 0.84; Fig. S4 D), which indicates that the effects of shootin1 overexpression on L1-dependent axon outgrowth are not affected by PI 3-kinase activity, as in the case of shootin1 RNAi. Thus, we considered that L1-dependent axon outgrowth induced by shootin1 was mediated mainly through a PI 3-kinase–independent mechanism. Together, these results suggest that enhancing the actin flow–L1 linkage by shootin1 overexpression promotes L1-dependent neurite outgrowth.

Discussion

Linkage between actin filament retrograde flow and CAMs in growth cones is thought to transmit the force of actin filament movement to extracellular substrates via CAMs, thereby providing mechanical tension for axonal outgrowth and guidance. Actin flow–CAM linkage has also been found to produce mechanical tension in nonneuronal cells (Felsenfeld et al., 1996) and has been implicated in cell migration (Felsenfeld et al., 1996) and the relocation of cell–cell contacts (Kametani and Takeichi, 2007). Concerning the actin flow–CAM linkage in growth cones, a critical question that remains to be addressed is the molecular basis for the linkage. It is also unknown whether coupling of this linkage induces axon outgrowth. Here, we have shown that shootin1 interacts with both actin filament retrograde flow and L1 in axonal growth cones and provided evidence that shootin1 mediates the linkage between them. When this linkage was impaired by shootin1 RNAi or NES-ΔN-shootin1, axon outgrowth was inhibited in an L1-dependent manner. However, enhancing the linkage by shootin1 overexpression promoted L1-dependent neurite outgrowth. We previously found that shoootin1 overexpression induced formation of multiple axons on coverslips coated with polylysine and laminin (Toriyama et al., 2006). As laminin binds to multiple CAMs, including L1 and its chicken relative NgCAM (Grumet et al., 1993; Brummendorf and Rathjen, 1996; Hall et al., 1997), we considered the fact that the coverslips coated with polylysine and laminin could monitor L1-dependent neurite outgrowth by shootin1. Collectively, the present results suggest that shootin1 is a key molecule involved in the actin flow–CAM linkage for axon outgrowth.

We do not rule out the involvement of other molecules in the linkage between actin filament flow and L1, or the possibility that shootin1 may couple actin flow to other CAMs. Unknown molecules may mediate the interaction between shootin1 and L1, as we could not obtain evidence that shootin1 directly interacts with L1. At present, it is also unknown whether shootin1 interacts directly with actin filaments or through association with other molecules. The velocity of L1-Fc–coated microbeads on growth cones was slower than those of shootin1 and actin filament retrograde flows. Therefore, the couplings between shootin1 and L1 may incorporate "clutchlike" slippages as previously proposed (Mitchison and Kirschner, 1988), or this may simply be reflective of the fact that the retrograde flow has to move a heavy bead. Recently, we detected phosphorylated forms of shootin1 in cultured hippocampal neurons (unpublished data). It will be intriguing to learn whether phosphorylation of shootin1 is involved in modulation of actin flow–CAM linkage, which has been implicated in regulation of axon outgrowth and guidance (Suter et al., 1998; Suter and Forscher, 2000). Detailed molecular mechanisms involved in actin filament–shootin1 linkage and shootin1-L1 linkage remain important issues for future analysis.

In conclusion, this study has shown that shootin1 mediates the linkage between actin filament retrograde flow and L1 in growth cones. Formation of this linkage together with multiple mechanisms involving actin polymerization near the leading edge (Mallavarapu and Mitchison, 1999), microtubule dynamics (Tanaka and Sabry, 1995; Dent and Gertler, 2003), axonal transport (Brown, 2003), and plasma membrane expansion (Lockerbie et al., 1991) may coordinately contribute to axon outgrowth.

Materials and methods

Cultures and transfection

Hippocampal neurons prepared from embryonic day 18 rat embryos were cultured on coverslips coated with L1-Fc, N-cadherin–Fc, or polylysine as described previously (Inagaki et al., 2001). They were transfected with vectors using Nucleofector (Amaxa) before plating. XTC cells were cultured as described previously (Higashida et al., 2004) and transfected with vectors using SuperFect (QIAGEN). Coverslips coated with polylysine, L1-Fc, or N-cadherin–Fc were prepared as described previously (Inagaki et al., 2001; Kamiguchi and Yoshihara, 2001).

DNA constructs

cDNA fragments of the shootin1 deletion mutants ΔN-shootin1 and ΔC-shootin1 were amplified by PCR and subcloned into pCAGGS-myc (Niwa et al., 1991) or pEGFP (Clontech Laboratories, Inc.) vectors. pCAGGS-myc was used to overexpress proteins under the β-actin promoter as described previously (Toriyama et al., 2006). Unexpectedly, myc-ΔN-shootin1 preferentially accumulated in the neuronal nucleus, whereas it was mainly localized in the cytoplasm of XTC cells. To express myc-ΔN-shootin1 in the cytoplasm of neurons, we fused the NES LSLKLAGLDL (Fukuda et al., 1996) to the N terminus of ΔN-shootin1. The RNAi refractory shootin1 mutant was generated by using QuikChange II site-directed mutagenesis kit (Stratagene). Four silent mutations (underlined) in 5′-TGAAGCTGTTAAAAA-GTTAGA-3′ were induced in the target sequence of shootin1 shRNA (Toriyama et al., 2006).

RNAi

Expression of shootin1 was suppressed using shRNA designated against shootin1 as described previously (Toriyama et al., 2006). The original vector to express shRNAs was designed to coexpress EGFP. We also constructed a vector that does not coexpress EGFP by deleting the coding sequence of EGFP. For vector-based RNAi of L1, we also used the BLOCK-iT Pol II miR RNAi Expression Vector kit (Invitrogen). The targeting mRNA sequence 5′-ATCATTCAGACTACATCTGCA-3′ corresponds to nucleotides 605–625 in the coding region of rat L1, whereas the control vector pcDNA 6.2-GW/EmGFP-miR-neg encodes an mRNA not to target any known vertebrate gene. To ensure a high-level expression of shRNA before neurite elongation, hippocampal neurons prepared from embryonic day 18 rat embryo and transfected with the expression vector shRNA were plated on uncoated polystyrene plates. After a 20-h incubation to induce shRNA expression, the cells were collected and cultured on coverslips coated with polylysine, L1-Fc, or N-cadherin–Fc. Reduction of shootin1 and L1 levels in neurons was confirmed immunocytochemically using anti-shoootin1 (Toriyama et al., 2006) and anti-L1 antibodies (Fig. S5, available at http://www.jcb.org/cgi/content/full/jcb.200712138/DC1).

Immunocytochemistry and immunoprecipitation

Immunocytochemistry and immunoprecipitation were performed as described previously (Toriyama et al., 2006). Secondary antibodies and phalloidin were conjugated with Alexa 488 (Invitrogen), Alexa 594 (Invitrogen),

or rhodamine (Invitrogen). We used 50% glycerol and 50% PBS as the mounting medium.

Microscopy

Fluorescence and phase-contrast images of fixed neurons were acquired at room temperature using a fluorescence microscope (Axioplan2; Carl Zeiss, Inc.) equipped with a plan-Neofluar 40× 0.75 NA or 20× 0.50 NA objective (Carl Zeiss, Inc.), a charge-coupled device camera (AxioCam MRm; Carl Zeiss, Inc.), and imaging software (Axiovision 3; Carl Zeiss, Inc.). The original images of shootin1 immunoreactivity and Alexa 594 phalloidin staining were quantified using Multi Gauge software (Fujifilm). Adjustments of image size, brightness, and contrast were performed on Photoshop Element 5.0 (Adobe). For the deconvolution analysis shown in Fig. 1 B and Fig. 3 A, z series of focal planes were digitally imaged at room temperature using a fluorescence microscope (Axiovert S100; Carl Zeiss, Inc.) equipped with a plan-Apochromat 63× oil 1.40 NA objective (Carl Zeiss, Inc.) and CSNAP and Deltavision2 (Applied Precision, LLC) software, and deconvolved with the Deltavision constrained iterative algorithm to generate high-resolution images.

Fluorescent speckle imaging

Fluorescent speckle imaging was performed as described previously (Watanabe and Mitchison, 2002) using EGFP- or mCherry-tagged proteins, and cells were cultured in Leibovitz's L-15 medium (Invitrogen). Speckle images were acquired at room temperature (XTC cells) or 37°C (neurons) using a fluorescent microscope (BX52; Olympus) equipped with a cooled charge-coupled device (CCD) camera (Cool SNAP HQ; Roper Scientific), or an inverted microscope (IX71; Olympus) equipped with a cooled CCD camera (UIC-QE; MDS Analytical Technologies), using in both cases a plan-Apochromat 100× oil 1.40 NA objective (Olympus) and imaging software (MetaMorph; MDS Analytical Technologies). Adjustments of image size, brightness, and contrast were performed on Photoshop Element 5.0. Speckle speed was measured by the following procedure, using Multi Gauge software. First, a pair of moving speckles that kept their relative position constant for at least 20 s during each experiment (5 frames) were identified. We then manually overlaid 300-nm-diameter circle scales on one of these speckles, and the translocation of the circles between the first and fifth frames was measured.

Bead tracking

1-μm-diameter polystyrene beads (Polysciences, Inc.) were coated with L1-Fc or anti-L1 antibody (Kamiguchi and Yoshihara, 2001) as described previously (Nishimura et al., 2003). To prepare polylysine-coated beads, a 1% (wt/vol) aqueous suspension of 1-μm-diameter polystyrene beads was mixed with an equal volume of 20 mg/ml carbodiimide in sodium phosphate buffer for 4 h at room temperature. After washes, the beads were incubated with 1 mg/ml polylysine in PBS, pH 7.4, overnight at room temperature. The beads were blocked with 7.5 mg/ml BSA in 50 mM Tris-HCl buffer, pH 8.0, and stored in PBS at 4°C. As described previously (Kamiguchi and Yoshihara, 2001), we used the laser optical trap system to place beads on growth cones cultured in Leibovitz's L-15 medium (Invitrogen).

As vectors expressing shRNAs are designed to coexpress EGFP, we used the EGFP fluorescence to identify growth cones expressing shRNA during bead tracking experiments. Reduction of shootin1 and L1 levels and expression of myc-tagged proteins in neurons were confirmed immunocytochemically after the experiments. Differential interference contrast (DIC) images of beads were acquired at room temperature using a fluorescence microscope (Eclipse TE2000-U; Nikon) equipped with a plan-Apochromat 60× WI 1.20 NA objective (Nikon) and a digital video camera (DCR-SR100; Sony). Videos were acquired directly by the video camera without software. Extraction of still images from videos was performed by Premier 6 (Adobe). Adjustments of image size, brightness, and contrast were performed on Photoshop Element 5.0. Bead velocity was quantified using Multi Gauge software. We manually overlaid 1-μm-diameter circle scales on the images of microbeads and then measured translocation of the scales during a 2-min observation period (121 frames).

Statistics

In the statistical analysis, significance was determined by the unpaired Student's *t* test.

Materials

Preparation of anti-shootin1 antibody has been described previously (Toriyama et al., 2006). Antibody against the L1 cytoplasmic domain (Schaefer et al., 1999) was provided by V. Lemmon (University of Miami School of Medicine, Miami, FL). Antibodies against myc and L1 were obtained from MBL International and Santa Cruz Biotechnology Inc., respectively. Blebbistatin, cytochalasin D, and poly-D-lysine were obtained from BIOMOL International, L.P., EMD, and Sigma-Aldrich, respectively. Rhodamine phalloidin and Alexa 594 phalloidin were obtained from Invitrogen. mCherry (Shaner et al., 2004) was provided by R. Tsien (University of California, San Diego, San Diego, CA).

Online supplemental material

Fig. S1 shows linkage between L1 and actin filament retrograde flow in axonal growth cones. Fig. S2 shows the effects of shootin1 RNAi and NES-ΔN-shootin1 overexpression on actin filament retrograde flow in axonal growth cones. Fig. S3 shows the effects of RNAi refractory shootin1 and LY294002 on the shootin1 RNAi–induced inhibition of axon outgrowth on L1-Fc. Fig. S4 shows the effects of shootin1 overexpression on actin filament retrograde flow together with the effects of LY294002 on the shootin1-induced promotion of L1-dependent neurite outgrowth. Fig. S5 shows repression of L1 by RNAi. Videos 1 and 5 are time-lapse videos of EGFP-shootin1 speckles in the growth cone of hippocampal neurons as described in Fig. 1 C and Fig. 2 B. Video 2 is a time-lapse video of EGFP-shootin1 speckles in an XTC cell as described in Fig. 1 D. Video 3 and 4 are time-lapse videos of EGFP-shootin1 and mCherry-actin speckles in XTC cells as described in Fig. 1 E and Fig. 2 A. Video 6 and 7 are time-lapse videos of L1-Fc–coated beads on the axonal growth cone of hippocampal neuron as described in Fig. 4 (A and B). Video 8 is a time-lapse video of EGFP-ΔN-shootin1 speckles in an XTC cell as described in Fig. 5 B. Video 9 is a time-lapse video of EGFP-shootin1 and mCherry-actin speckles in the same XTC cell as described in Fig. 5 C. Online supplemental material is available at http://www.jcb.org/cgi/content/full/jcb.200712138/DC1.

We thank V. Lemmon for providing anti-L1 antibody and L1 constructs, R. Tsien for providing mCherry, A. Konishi for discussion, and I. Smith for reviewing the manuscript.

This research was supported in part by the Ministry of Education, Culture, Sports, Science and Technology (MEXT; 20300111 and 19700291) and the Japan Society for the Promotion of Science (20022029 and 20016017) Grant-in-Aid for Scientific Research, the Global Centers of Excellence Program at Nara Institute of Science and Technology (MEXT), the Osaka Medical Research Foundation for Incurable Diseases, and the Nara Institute of Science and Technology Interdisciplinary Promotion Project.

Submitted: 21 December 2007
Accepted: 30 April 2008

References

Bray, D. 1979. Mechanical tension produced by nerve cells in tissue culture. *J. Cell Sci.* 37:391–410.

Bray, D., and P.J. Hollenbeck. 1988. Growth cone motility and guidance. *Annu. Rev. Cell Biol.* 4:43–61.

Brown, A. 2003. Axonal transport of membranous and nonmembranous cargoes: a unified perspective. *J. Cell Biol.* 160:817–821.

Brummendorf, T., and F.G. Rathjen. 1996. Structure/function relationships of axon-associated adhesion receptors of the immunoglobulin superfamily. *Curr. Opin. Neurobiol.* 6:584–593.

Dahme, M., U. Bartsch, R. Martini, B. Anliker, M. Schachner, and N. Mantei. 1997. Disruption of the mouse L1 gene leads to malformations of the nervous system. *Nat. Genet.* 17:346–349.

Dent, E.W., and F.B. Gertler. 2003. Cytoskeletal dynamics and transport in growth cone motility and axon guidance. *Neuron.* 40:209–227.

Diefenbach, T.J., V.M. Latham, D. Yimlamai, C.A. Liu, I.M. Herman, and D.G. Jay. 2002. Myosin 1c and myosin IIB serve opposing roles in lamellipodial dynamics of the neuronal growth cone. *J. Cell Biol.* 158:1207–1217.

Faivre-Sarrailh, C., J. Falk, E. Pollerberg, M. Schachner, and G. Rougon. 1999. NrCAM, cerebellar granule cell receptor for the neuronal adhesion molecule F3, displays an actin-dependent mobility in growth cones. *J. Cell Sci.* 112:3015–3027.

Felsenfeld, D.P., D. Choquet, and M.P. Sheetz. 1996. Ligand binding regulates the directed movement of beta1 integrins on fibroblasts. *Nature.* 383:438–440.

Forscher, P., and S.J. Smith. 1988. Actions of cytochalasins on the organization of actin filaments and microtubules in a neuronal growth cone. *J. Cell Biol.* 107:1505–1516.

Fukuda, M., I. Gotoh, Y. Gotoh, and E. Nishida. 1996. Cytoplasmic localization of mitogen-activated protein kinase kinase directed by its NH2-terminal,

leucine-rich short amino acid sequence, which acts as a nuclear export signal. *J. Biol. Chem.* 271:20024–20028.

Gil, O.D., T. Sakurai, A.E. Bradley, M.Y. Fink, M.R. Cassella, J.A. Kuo, and D.P. Felsenfeld. 2003. Ankyrin binding mediates L1CAM interactions with static components of the cytoskeleton and inhibits retrograde movement of L1CAM on the cell surface. *J. Cell Biol.* 162:719–730.

Grabham, P.W., M. Foley, A. Umeojiako, and D.J. Goldberg. 2000. Nerve growth factor stimulates coupling of beta1 integrin to distinct transport mechanisms in the filopodia of growth cones. *J. Cell Sci.* 113:3003–3012.

Grumet, M., D.R. Friedlander, and G.M. Edelman. 1993. Evidence for the binding of Ng-CAM to laminin. *Cell Adhes. Commun.* 1:177–190.

Hall, H., S. Carbonetto, and M. Schachner. 1997. L1/HNK-1 carbohydrate- and beta 1 integrin-dependent neural cell adhesion to laminin-1. *J. Neurochem.* 68:544–553.

Higashida, C., T. Miyoshi, A. Fujita, F. Oceguera-Yanez, J. Monypenny, Y. Andou, S. Narumiya, and N. Watanabe. 2004. Actin polymerization-driven molecular movement of mDia1 in living cells. *Science.* 303:2007–2010.

Inagaki, N., K. Chihara, N. Arimura, C. Menager, Y. Kawano, N. Matsuo, T. Nishimura, M. Amano, and K. Kaibuchi. 2001. CRMP-2 induces axons in cultured hippocampal neurons. *Nat. Neurosci.* 4:781–782.

Jay, D.G. 2000. The clutch hypothesis revisited: ascribing the roles of actin-associated proteins in filopodial protrusion in the nerve growth cone. *J. Neurobiol.* 44:114–125.

Kametani, Y., and M. Takeichi. 2007. Basal-to-apical cadherin flow at cell junctions. *Nat. Cell Biol.* 9:92–98.

Kamiguchi, H., and F. Yoshihara. 2001. The role of endocytic L1 trafficking in polarized adhesion and migration of nerve growth cones. *J. Neurosci.* 21:9194–9203.

Kamiguchi, H., M.L. Hlavin, M. Yamasaki, and V. Lemmon. 1998. Adhesion molecules and inherited diseases of the human nervous system. *Annu. Rev. Neurosci.* 21:97–125.

Katoh, K., K. Hammar, P.J. Smith, and R. Oldenbourg. 1999. Birefringence imaging directly reveals architectural dynamics of filamentous actin in living growth cones. *Mol. Biol. Cell.* 10:197–210.

Lamoureux, P., R.E. Buxbaum, and S.R. Heidemann. 1989. Direct evidence that growth cones pull. *Nature.* 340:159–162.

Lemmon, V., K.L. Farr, and C. Lagenaur. 1989. L1-mediated axon outgrowth occurs via a homophilic binding mechanism. *Neuron.* 2:1597–1603.

Lin, C.H., and P. Forscher. 1995. Growth cone advance is inversely proportional to retrograde F-actin flow. *Neuron.* 14:763–771.

Lockerbie, R.O., V.E. Miller, and K.H. Pfenninger. 1991. Regulated plasmalemmal expansion in nerve growth cones. *J. Cell Biol.* 112:1215–1227.

Mallavarapu, A., and T. Mitchison. 1999. Regulated actin cytoskeleton assembly at filopodium tips controls their extension and retraction. *J. Cell Biol.* 146:1097–1106.

Medeiros, N.A., D.T. Burnette, and P. Forscher. 2006. Myosin II functions in actin-bundle turnover in neuronal growth cones. *Nat. Cell Biol.* 8:215–226.

Mitchison, T., and M. Kirschner. 1988. Cytoskeletal dynamics and nerve growth. *Neuron.* 1:761–772.

Nishimura, K., F. Yoshihara, T. Tojima, N. Ooashi, W. Yoon, K. Mikoshiba, V. Bennett, and H. Kamiguchi. 2003. L1-dependent neuritogenesis involves ankyrinB that mediates L1-CAM coupling with retrograde actin flow. *J. Cell Biol.* 163:1077–1088.

Niwa, H., K. Yamamura, and J. Miyazaki. 1991. Efficient selection for high-expression transfectants with a novel eukaryotic vector. *Gene.* 108:193–199.

Oliva, A.A. Jr., C.D. James, C.E. Kingman, H.G. Craighead, and G.A. Banker. 2003. Patterning axonal guidance molecules using a novel strategy for microcontact printing. *Neurochem. Res.* 28:1639–1648.

Ramon y Cajal, S.R. 1890. À quelle époque apparaissent les expansions des cellules nerveuses de la moëlle épinière du poulet. *Anatomischer Anzeiger.* 5:609–613.

Schaefer, A.W., H. Kamiguchi, E.V. Wong, C.M. Beach, G. Landreth, and V. Lemmon. 1999. Activation of the MAPK signal cascade by the neural cell adhesion molecule L1 requires L1 internalization. *J. Biol. Chem.* 274:37965–37973.

Shaner, N.C., R.E. Campbell, P.A. Steinbach, B.N. Giepmans, A.E. Palmer, and R.Y. Tsien. 2004. Improved monomeric red, orange and yellow fluorescent proteins derived from *Discosoma* sp. red fluorescent protein. *Nat. Biotechnol.* 22:1567–1572.

Suter, D.M., and P. Forscher. 2000. Substrate-cytoskeletal coupling as a mechanism for the regulation of growth cone motility and guidance. *J. Neurobiol.* 44:97–113.

Suter, D.M., L.D. Errante, V. Belotserkovsky, and P. Forscher. 1998. The Ig superfamily cell adhesion molecule, apCAM, mediates growth cone steering by substrate-cytoskeletal coupling. *J. Cell Biol.* 141:227–240.

Tanaka, E., and J. Sabry. 1995. Making the connection: cytoskeletal rearrangements during growth cone guidance. *Cell.* 83:171–176.

Toriyama, M., T. Shimada, K.B. Kim, M. Mitsuba, E. Nomura, K. Katsuta, Y. Sakumura, P. Roepstorff, and N. Inagaki. 2006. Shootin1: a protein involved in organization of an asymmetric signal for neuronal polarization. *J. Cell Biol.* 175:147–157.

Watanabe, N., and T.J. Mitchison. 2002. Single-molecule speckle analysis of actin filament turnover in lamellipodia. *Science.* 295:1083–1086.

Waterman-Storer, C.M., and E.D. Salmon. 1997. Actomyosin-based retrograde flow of microtubules in the lamella of migrating epithelial cells influences microtubule dynamic instability and turnover and is associated with microtubule breakage and treadmilling. *J. Cell Biol.* 139:417–434.